A&A 568, A32 (2014)
DOI: 10.1051/0004-6361/201423478

Astronomy & Astrophysics

Searching for δ Scuti-type pulsation and characterising northern pre-main-sequence field stars

D. Díaz-Fraile, E. Rodríguez, and P. J. Amado

Instituto de Astrofísica de Andalucía, CSIC, P.O. 3004, 18080 Granada, Spain
e-mail: dario@iaa.es

Received 21 January 2014 / Accepted 17 June 2014

ABSTRACT

Context. Pre-main-sequence (PMS) stars are objects evolving from the birthline to the zero-age main sequence (ZAMS). Given a mass range near the ZAMS, the temperatures and luminosities of PMS and main-sequence stars are very similar. Moreover, their evolutionary tracks intersect one another causing some ambiguity in the determination of their evolutionary status. In this context, the detection and study of pulsations in PMS stars is crucial for differentiating between both types of stars by obtaining information of their interiors via asteroseismic techniques.

Aims. A photometric variability study of a sample of northern field stars, which previously classified as either PMS or Herbig Ae/Be objects, has been undertaken with the purpose of detecting δ Scuti-type pulsations. Determination of physical parameters for these stars has also been carried out to locate them on the Hertzsprung-Russell diagram and check the instability strip for this type of pulsators.

Methods. Multichannel photomultiplier and CCD time series photometry in the *uvby* Strömgren and *BVI* Johnson bands were obtained during four consecutive years from 2007 to 2010. The light curves have been analysed, and a variability criterion has been established. Among the objects classified as variable stars, we have selected those which present periodicities above 4 d^{-1}, which was established as the lowest limit for δ Scuti-type pulsations in this investigation. Finally, these variable stars have been placed in a colour–magnitude diagram using the physical parameters derived with the collected $uvby\beta$ Strömgren-Crawford photometry.

Results. Five PMS δ Scuti- and three probable β Cephei-type stars have been detected. Two additional PMS δ Scuti stars are also confirmed in this work. Moreover, three new δ Scuti- and two γ Doradus-type stars have been detected among the main-sequence objects used as comparison or check stars.

Key words. asteroseismology – stars: pre-main sequence – stars: variables: T Tauri, Herbig Ae/Be – stars: variables: δ Scuti – stars: fundamental parameters – Hertzsprung-Russell and C-M diagrams

1. Introduction

Pre-main-sequence (PMS) stars are objects that evolve from the birthline, which is the locus in the Hertzsprung-Russell diagram along which young stars first appear as optically visible objects (Stahler 1983), to the zero-age main sequence (ZAMS). They are observed both in the field, mainly in the vicinity of molecular clouds, and in young open clusters with spectral types between late B and late M. In the case of PMS field stars, they are characterised by a high degree of activity, strong IR excess caused by the presence of circumstellar material, and emission lines in most cases. They show photometric and spectroscopic variability due to the photospheric activity and interaction with the circumstellar medium. These observational characteristics classify them as either T Tauri stars (Joy 1945; Herbig 1962) when their spectral types are later than F or as Herbig Ae/Be (HAEBE) objects (Herbig 1960; Finkenzeller & Mundt 1984) when their spectral types are in the early F to late B range.

Close to the ZAMS, the evolutionary tracks of PMS and post-main-sequence stars intersect each other several times (Breger & Pamyatnykh 1998). Therefore, their evolutionary status is ambiguous at a given combination of effective temperature ($T_{\rm eff}$), luminosity ($L/L_{\odot}$), and mass ($M_{\odot}$). The PMS stars only differ from their counterparts on the main-sequence (MS) in their interiors, whereas their atmosphere properties are very similar (Marconi & Palla 1998).

In their contraction phase towards the ZAMS, PMS stars with intermediate masses, i.e., between ~1.5 and 4 $M_{\odot}$, cross the classical instability strip, where δ Scuti-type pulsations can be excited. Several pulsating PMS stars have been discovered and studied within the last few years (Zwintz 2008; Zwintz et al. 2009). Their pulsation periods range between 18 min (80 d^{-1}; Amado et al. 2004) and about 6 h (4 d^{-1}) with amplitudes usually of only a few millimagnitudes (Rodríguez & Breger 2001). As the pulsational properties depend on the inner structure of the stars, the detection of δ Scuti-type pulsations is particularly important to discriminate between both different evolutionary stages and the modelling of their interiors using asteroseismic techniques (Guenther et al. 2007, 2009; Zwintz et al. 2011, 2013).

The main aim of this work was to conduct a search for δ Scuti-type pulsations over a sample of northern field stars that are brighter than $V \approx 13\overset{\rm m}{.}0$, which are previously classified as either PMS or HAEBE stars. This previous classification comes from different sources; they mainly come from the The et al. (1994) and Vieira et al. (2003) HAEBE catalogues and the list with all known PMS pulsators and pulsating candidate stars by Zwintz (2008). An initial sample of 63 stars was selected, which includes all PMS and HAEBE field stars known to date and visible from the northern hemisphere. However, four stars (UX Ori, HD 34282, V436 Ori, and V351 Ori) were rejected from the sample because they had already been studied properly in the literature.

The paper is organized as follows. The observations and data reduction are described in Sect. 2. Frequency analysis and results obtained are described in Sects. 3−5. Section 6 is devoted to the determination of the stellar physical parameters and to locating the stars in a colour-magnitude diagram. The summary and the main conclusions are given in Sect. 7.

2. Observations and data reduction

The sample was observed photometrically between the years 2007 and 2010 using the 1.5 m (T150) and 0.9 m (T90) telescopes at Sierra Nevada Observatory (SNO), Granada, Spain. In the case of T150, Johnson *BVI* filters were used with CCD imaging for stars that are fainter than $V \approx 10\overset{\mathrm{m}}{.}5$. In the case of T90 for stars brighter than $V \approx 10\overset{\mathrm{m}}{.}5$, simultaneous multicolour Strömgren *uvby* photometry was carried out using the six-channel *uvby* photometer (Strömgren photometer) that is attached to this telescope (Rodríguez et al. 1997). This magnitude value was established as the limit for the T90 for providing sufficient precision in searching for very-low-amplitude pulsations. Nevertheless, all stars (except RR Tau, see Table 7) were observed with the Strömgren photometer to obtain their $uvby\beta$ indices for calibration purposes. In Table 1, the list of ID numbers for each object is provided (ID numbers 7, 8, 11, and 29 correspond to UX Ori, HD 34282, V436 Ori, and V351 Ori, respectively, are not included in the Table, see Sect. 1) with *V* magnitudes, coordinates (J2000), and spectral types obtained from the literature. Basic information about the observations carried out for the 59 PMS stars in our sample is also provided there. In total, photometric data have been acquired on 136 nights (78 nights on T90 and 58 nights on T150) by obtaining 480 h of observation (238 h on T90 and 197 h on T150) and collecting 12 823 data points (4261 points on T90 and 8562 points on T150). Traditional criteria of proximity, similar brightness, and spectral types were applied when selecting the comparison and check stars in the case of observations with T90 and Strömgren photometer. The same selection criteria were applied to T150 observations but for stars within the CCD FoV.

The atmospheric extinction correction was based on nightly coefficients determined from the main comparison star in each case. Magnitude differences were also calculated relative to the main comparison star by means of linear interpolation. For T90 data, instrumental magnitude differences were transformed into a standard $uvby\beta$ system following the procedure described in Rodríguez et al. (1997). The T150 data were reduced with IRAF[1] software package following the standard procedure. Dates of observations were converted to the Heliocentric Julian Date (HDJ), and the zero point in time was set to the beginning of the observations for each observed star.

3. Frequency analysis

The HAEBE stars usually show large variations in luminosity from one year to another with an irregular (or at least not periodic) pattern due to the presence of circumstellar material (Wenzel et al. 1971; Grinin et al. 1994; Herbst & Shevchenko 1999; Oudmaijer et al. 2001). This long-term variability was removed from the whole data set for each star fitting a low-order Legendre polynomial. The residuals were then used to study their pulsational behaviour.

The program package PERIOD04 (Lenz & Breger 2005) was used to perform the frequency analysis. The time interval between samples is about 3 min (T90) or 5 min (T150), which leads to a Nyquist frequency of $f_{\rm Nyq}$ ∼250 d^{-1} or $f_{\rm Nyq}$ ∼ 150 d^{-1}, respectively. The frequency spectra were first studied in the *v* and *B* bands because of the higher flux and pulsational amplitudes in A-F stars. The frequency range was selected from 0 to 100 d^{-1} to include the highest frequencies predicted by models and observed in a PMS star (Casey et al. 2013). The 1σ noise level was determined by computing the mean noise amplitude in that range. Based on this value, 3σ and 4σ levels were calculated in each case. Our variability criterion was established as follows:

- Peaks with an amplitude larger than 4σ level are considered as real peaks, and these stars as variable stars.
- Peaks between 3σ and 4σ levels are considered as doubtful, and the variability of the star as uncertain.
- Peaks below 3σ level are considered as not significant and the star as not variable.

In the particular cases of stars with their main frequency peaks showing amplitudes between 3σ and 4σ levels, the *Time Resolved Image Photometry Package* (TRIPP, Schuh et al. 2003) was also used to check the results obtained with PERIOD04. This package computes a Lomb-Scargle periodogram (Scargle 1982) instead of a Fourier amplitude spectrum. The program TRIPP provides a statistical estimate of the probability of a peak being real by using confidence levels for the relative power. It was established that those peaks between 3σ and 4σ levels with a confidence ≥95% are considered as real peaks, and the star would be considered as variable. Following this criterion, we have found that 26 stars from our sample show some type of variability. We note that our limit of 4σ is similar to that with an amplitude signal-to-noise ratio $S/N = 4.0$, which is commonly accepted for this type of works (Breger et al. 1993, 1999).

Tables 2 and 3 show the results obtained from the frequency analysis: object name, spectral type, visual magnitude, frequencies detected, amplitudes, mean noise level, and signal-to-noise ratio. Table 3 includes the results obtained with *TRIPP* that shows the probability that the frequency detected would be real. In all cases, the frequencies, amplitudes, and S/N values listed correspond to the analysis obtained from Johnson *B* (T150) or Strömgren *v* (T90) bands. Frequency and amplitude errors are indicated in the parentheses that correspond to the last digits. They are the formal error bars given by PERIOD04, which are computed using the formulae derived by Montgomery & O'Donoghue (1999). Nevertheless, the calculated errors in frequency are very small because the stars were observed during very few nights spanning in time over different years in most of the stars in our study. This leads to unreliably small error bars in frequency. In these cases, we assume that the errors in our frequency determinations are much larger, typically of about 0.01 d^{-1}.

To establish the type of variability and discriminate between an intrinsic pulsation of the star and an external effect, such as luminosity variations produced by the circumstellar material commonly present around this type of HAEBE star, a more detailed analysis of all the different bands (*uvby* or *BVI*) was carried out and is described in the next section.

[1] The Image Reduction and Analysis Facility (IRAF) is distributed by the National Optical Astronomy Observatories, which are operated by Association of Universities for Research in Astronomy, Inc., under cooperative agreement with the National Science Foundation.

Table 1. Full sample of observed HAEBE and PMS field stars.

ID Number	Name	α (J2000)	δ (J2000)	V (mag)	Spectral Type	Telescope SNO	Season	Hours (nights)	Points
1	VX Cas	00 31 30.68	+61 58 50.97	11.30	A0	T150	Aug. 07	3.10 (1)	220
						T150	Nov. 07	4.15 (1)	58
2	V594 Cas	00 43 18.25	+61 54 40.14	10.64	Be	T150	Aug. 07	6.03 (1)	392
3	PDS 004	03 39 00.56	+29 41 45.70	10.74	A1	T150	Nov. 07	2.21 (1)	68
						T150	Nov. 08	3.96 (1)	208
						T90	Dec. 09	4.62 (1)	68
4	XY Per	03 49 36.32	+38 58 55.60	9.44	A2II	T90	Oct. 07	3.50 (1)	57
						T90	Dec. 09	2.38 (1)	37
5	AB Aur	04 55 45.84	+30 33 04.29	7.06	A0Vpe	T90	Oct. 07	2.91 (1)	38
6	HD 31648	04 58 46.26	+29 50 36.98	7.73	A3	T90	Oct. 07	3.02 (1)	39
9	HD 35187	05 24 01.17	+24 57 37.58	7.78	A2e	T90	Oct. 07	8.46 (2)	184
						T90	Dec. 07	1.41 (1)	37
						T90	Dec. 09	3.39 (1)	64
10	HD 287823	05 24 08.05	+02 27 46.89	9.67	A0	T90	Nov. 07	2.91 (1)	32
12	HD 290409	05 27 05.47	+00 25 07.61	9.96	B9	T90	Nov. 07	2.92 (1)	33
13	HD 290500	05 29 48.03	−00 23 43.16	11.04	B8	T150	Nov. 07	2.33 (1)	44
						T150	Nov. 08	3.49 (1)	119
						T150	Oct. 09	3.17 (1)	156
14	V1409 Ori	05 30 19.03	+11 20 19.90	9.30	A1ab	T90	Oct. 07	4.94 (1)	69
						T90	Nov. 07	5.94 (2)	131
						T90	Dec. 09	4.07 (1)	68
15	HD 36112	05 30 27.53	+25 19 57.08	8.31	A3e	T90	Oct. 07	8.38 (2)	114
						T90	Dec. 07	1.32 (1)	18
						T90	Dec. 09	8.32 (1)	153
16	V1410 Ori	05 31 57.24	+11 17 41.46	9.43	A3	T90	Oct. 07	4.94 (1)	63
						T90	Nov. 07	2.72 (1)	28
17	HD 36408	05 32 14.14	+17 03 29.25	5.46	B7IIIe	T90	Oct. 07	5.61 (1)	75
						T90	Nov. 07	3.11 (1)	75
18	V1271 Ori	05 35 09.60	+10 01 51.51	10.00	A5	T90	Oct. 07	5.62 (1)	73
19	V380 Ori	05 36 25.43	−06 42 57.69	10.70	A1e	T150	Nov. 07	2.81 (1)	45
20	HD 290770	05 37 02.45	−01 37 21.36	9.30	B8	T90	Nov. 07	2.42 (1)	31
21	BF Ori	05 37 13.26	−06 35 00.58	10.30	A5II-IIIe	T90	Oct. 07	1.58 (1)	13
						T90	Nov. 07	9.61 (2)	138
22	HD 37357	05 37 47.08	−06 42 30.25	8.85	A0e	T90	Oct. 07	5.58 (1)	58
23	V1247 Ori	05 38 05.25	−01 15 21.67	9.82	A5III	T90	Nov. 07	2.33 (1)	30
24	V1788 Ori	05 38 14.50	−05 25 13.30	9.86	B9Ve	T90	Nov. 07	5.13 (1)	57
25	RR Tau	05 39 30.52	+26 22 26.97	10.90	A2II-IIIe	T150	Nov. 07	1.26 (1)	34
						T150	Nov. 08	1.86 (1)	70
26	V350 Ori	05 40 11.77	−09 42 11.05	10.40	A0	T150	Jan. 08	5.24 (1)	270
						T150	Nov. 08	2.23 (1)	83
27	HD 37806	05 41 02.29	−02 43 00.73	7.93	A0	T90	Dec. 07	5.30 (1)	67
						T90	Feb. 10	1.71 (1)	21
28	HD 38120	05 43 11.89	−04 59 49.90	9.08	A0	T90	Dec. 07	5.27 (1)	66
						T90	Feb. 10	1.63 (1)	20
30	HD 249879	05 58 55.78	+16 39 57.37	10.64	B8	T150	Jan. 08	8.04 (1)	649
						T150	Nov. 08	3.69 (1)	295
						T150	Apr. 10	0.86 (1)	74
31	V791 Mon	06 02 14.88	−10 00 59.50	9.60	Be	T90	Feb. 08	5.38 (2)	149
						T90	Feb. 10	2.03 (1)	31
32	HD 250550	06 01 59.00	+16 30 56.73	9.57	B7e	T90	Feb. 08	4.86 (2)	118
						T90	Feb. 10	2.24 (1)	35
33	AE Lep	06 03 37.06	−14 53 02.50	11.00	Ae	T150	Jan. 08	5.27 (2)	358
						T150	Nov. 08	4.05 (1)	185
34	PDS 126	06 13 36.20	−06 25 01.00	11.82	A7V	T150	Jan. 08	6.61 (1)	218
35	HD 50083	06 51 45.75	+05 05 03.86	6.91	B2Ve	T90	Dec. 07	5.36 (2)	115
						T90	Feb. 08	2.84 (1)	101
						T90	Feb. 10	3.08 (1)	45
36	HD 52721	07 01 49.51	−11 18 03.32	6.58	B2Ve?	T90	Feb. 08	8.40 (2)	112
						T90	Feb. 10	1.00 (1)	9

Table 1. continued.

ID Number	Name	α (J2000)	δ (J2000)	V (mag)	Spectral Type	Telescope SNO	Season	Hours (nights)	Points
37	HT Cma	07 02 42.53	−11 26 11.81	11.87	A0	T150	Feb. 11	3.42 (1)	149
38	HU Cma	07 04 06.70	−11 26 08.61	12.09	B9e	T150	Feb. 08	4.06 (1)	187
39	HD 53367	07 04 25.53	−10 27 15.74	7.04	B0IV:e	T90	Feb. 08	8.41 (2)	117
						T90	Feb. 10	1.00 (1)	9
40	PDS 241	07 08 38.80	−04 19 08.00	12.06	B0?	T150	Jan. 08	6.03 (2)	151
						T150	Nov. 08	5.52 (1)	196
						T150	Apr. 10	1.21 (1)	60
41	HD 141569	15 49 57.75	−03 55 16.34	7.13	B9.5e	T90	Apr. 07	5.54 (1)	93
						T90	Feb. 10	1.55 (1)	27
42	VV Ser	18 28 47.86	+00 08 39.76	11.60	B6	T150	Apr. 07	7.01 (3)	136
						T150	Apr. 10	1.75 (1)	69
43	V431 Sct	18 29 25.69	−06 04 37.29	10.50	Bpe	T90	Jul. 07	6.06 (2)	85
						T150	Aug. 07	4.92 (2)	204
						T150	Apr. 10	1.45 (2)	41
44	HD 174571	18 50 47.18	+08 42 10.09	8.84	B3V:pe	T90	May 07	4.15 (1)	32
						T90	Jul. 07	3.92 (1)	60
						T90	Aug. 09	3.43 (1)	59
						T90	Apr. 10	2.62 (1)	25
45	HD 179218	19 11 11.25	+15 47 15.64	8.84	B9e	T90	May 07	6.13 (2)	47
						T90	Jul. 07	3.92 (1)	60
						T90	Apr. 10	2.59 (1)	24
46	WW Vul	19 25 58.75	+21 12 31.28	10.51	A3e	T150	May 07	2.73 (1)	129
						T150	Aug. 07	6.61 (1)	352
						T150	Aug. 09	1.15 (1)	63
						T150	Apr. 10	1.73 (1)	84
47	PX Vul	19 26 40.26	+23 53 50.85	11.67	F0V:e	T150	Aug. 07	4.52 (1)	127
						T150	Aug. 09	2.78 (2)	80
						T150	Apr. 10	1.72 (1)	61
48	PDS 581	19 36 18.91	+29 32 50.00	11.67	B0.sIV	T150	Aug. 07	4.55 (1)	80
						T150	Sep. 07	5.34 (1)	147
						T150	Apr. 10	2.05 (1)	75
49	HD 190073	20 03 02.51	+05 44 16.67	7.82	A2IVpe	T90	Jul. 07	2.97 (1)	45
50	V1685 Cyg	20 20 28.24	+41 21 51.56	10.70	B2	T150	Aug. 07	4.83 (1)	225
						T150	Aug. 09	5.24 (2)	238
51	HD 200775	21 01 36.92	+68 09 47.76	7.42	B2Ve	T90	May 07	4.39 (1)	49
						T90	Jul. 07	4.20 (1)	46
52	HD 203024	21 16 03.02	+68 54 52.13	8.88	A	T90	May 07	4.39 (1)	50
						T90	Jul. 07	4.20 (1)	47
53	BD +65.1637	21 42 50.18	+66 06 35.12	10.17	B2nne	T90	Jul. 07	8.91 (2)	146
54	V1578 Cyg	21 52 34.10	+47 13 43.61	10.16	B9.5Ve	T90	Jul. 07	9.87 (2)	165
						T150	Aug. 07	7.22 (1)	606
55	BH Cep	22 01 42.87	+69 44 36.53	10.8	F5IV	T150	Aug. 07	4.99 (1)	261
						T150	Nov. 07	3.77 (1)	67
						T150	Aug. 09	2.57 (1)	106
56	SV Cep	22 21 33.20	+73 40 27.07	10.10	Ae	T90	Jul. 07	4.29 (1)	72
57	V1080 Tau	04 40 32.64	+24 26 31.30	10.50	G0	T150	Nov. 07	5.17 (1)	98
58	CO Ori	05 27 38.34	+11 25 38.97	10.60	G5Vpe	T150	Nov. 07	5.01 (1)	94
						T150	Nov. 08	3.14 (1)	115
59	V1650 Ori	05 29 11.44	−06 08 05.41	10.43	F7	T90	Nov. 07	5.13 (1)	57
60	RY Ori	05 32 09.94	−02 49 46.79	10.80	F7	T150	Nov. 07	2.91 (1)	36
61	HD 36910	05 35 58.47	+24 44 54.10	10.70	F2IVe	T90	Oct. 07	3.63 (1)	58
62	HD 53240	07 03 57.45	−10 07 25.55	6.43	B9IIIn	T90	Feb. 08	8.28 (2)	106
63	HD 261387	06 39 20.79	+09 33 51.00	10.60	A2V	T90	Dec. 07	6.87 (1)	110
						T150	Jan. 08	6.14 (2)	429
						T150	Nov. 08	2.98 (1)	169
						T150	Apr. 10	2.40 (1)	181

Table 2. Stars of the sample with $S/N \geq 4.0$.

ID number	Name	Spectral Type	V (mag)	Frequency (d^{-1})	Amplitude (mmag)	N (mmag)	S/N
2	V594 Cas	Be	10.64	3.98 (11)	9.7 (5)	1.2	8.1
3	PDS 004	A1	10.74	53.27 (1)	8.5 (7)	2.0	4.2
4	XY Per	A2IIv	9.44	5.27 (1)	4.4 (5)	0.8	5.5
9	HD 35187	A2e	7.78	63.87 (1)	3.3 (4)	0.7	4.7
14	V1409 Ori	AIab	10.20	45.35 (1)	7.8 (7)	1.2	6.5
				2.43 (1)	6.5 (5)	1.2	5.4
15	HD 36112	A3e	8.31	28.36 (1)	3.7 (3)	0.5	7.4
				33.00 (1)	2.6 (3)	0.5	5.2
32	HD 250550	B7e	9.57	5.48 (1)	4.3 (4)	0.8	5.4
36	HD 52721	B2Ve?	6.58	3.51 (1)	80.7 (23)	9.0	9.0
40	PDS 241	B0?	12.06	2.86 (1)	4.6 (4)	0.8	5.7
42	VV Ser	A2e	11.60	9.65 (4)	2.8 (4)	0.5	5.6
43	V431 Sct	Bpe	10.50	11.66 (5)	6.8 (9)	1.0	6.8
44	HD 174571	B3V:pe	8.84	4.51 (1)	4.7 (4)	0.6	7.8
46	WW Vul	A3e	10.51	4.30 (1)	4.8 (5)	0.9	5.3
48	PDS 581	B0.sIV	11.67	6.83 (1)	4.8 (5)	0.5	9.6
50	V1685 Cyg	B3	10.70	7.10 (1)	4.0 (4)	0.8	5.0
55	BH Cep	F5IV	10.80	5.57 (1)	2.9 (3)	0.5	5.8
57	V1080 Tau	G0	10.50	2.86 (7)	22.5 (6)	3.0	7.5
59	V1650 Ori	F7	10.43	3.04 (12)	67.0 (30)	9.0	7.4
61	HD 36910	F2IVe	10.70	2.81 (4)	68.0 (40)	8.1	8.4
63	HD 261387	A2V	10.60	34.67 (1)	2.7 (3)	0.6	4.5

Table 3. Stars of the sample with $3.0 < S/N < 4.0$.

ID number	Name	Spectral Type	V (mag)	Frequency (d^{-1})	Amplitude (mmag)	N (mmag)	S/N	Prob. (%)
6	HD 31648	A3	7.73	5.60 (70)	3.8 (6)	1.2	3.2	98
13	HD 290500	B8	11.04	8.18 (1)	4.8 (7)	1.5	3.2	>99
17	HD 36408	B7IIIe	5.46	15.47 (2)	2.0 (4)	0.6	3.3	20
21	BF Ori	A5II-IIIeV	10.30	5.62 (1)	11.4 (16)	3.3	3.4	>99
26	V350 Ori	A0	10.40	57.08 (1)	3.3 (4)	0.9	3.7	>99
35	HD 50083	B2III	6.91	6.45 (1)	2.7 (3)	0.7	3.8	>99
45	HD 179218	B9e	8.84	4.81 (1)	1.5 (3)	0.4	3.7	0
58	CO Ori	G5Vpe	10.60	5.34 (1)	2.7 (4)	0.7	3.8	>99

4. Pulsating PMS field stars

We have found that five stars show δ Scuti-type pulsations (PDS 004, HD 35187, V1409 Ori, HD 36112, and V350 Ori). In addition, two other stars (HD 261387 and VV Ser) have also been confirmed as δ Scuti-type pulsators. The results are summarised in Table 4. Frequency and amplitude errors are indicated in parentheses. These stars fulfill the variability criterion in all the bands observed, whereas the rest of the stars that are listed in Tables 2 and 3 do not. Therefore, it is assumed that the peaks found in these latter objects are not caused by real variability. Figure 1 shows the results of the frequency analysis performed in the v or B bands for the PMS δ Scuti-type stars detected or confirmed.

On the other hand, three new MS δ Scuti- and two new MS γ Doradus-type stars have also been detected among the comparison and check stars. After a few hours, changes in the luminosities of these stars were revealed as evident with probable pulsational periodicities. Thus, these stars were rejected as comparison or check stars and re-observed to confirm the periodicities. In all cases, they were discovered using the T90 and *uvby* photometry. Figure 3 shows the respective amplitude spectra in the Strömgren v band for the new variables. Table 6 shows the results obtained from the frequency analysis and some basic information of the observations carried out for each star. The last column indicates the ID numbers of the objects to which these comparison and check stars were initially associated.

4.1. PDS 004

The object PDS 004 was observed at 2.21 and 3.96 h on two different nights in November 2007 and 2008, respectively, with T150 in the *BVI* bands. Additionally, it was observed at 4.62 h on only one night in December 2009 with T90 and Strömgren *uvby* bands. It shows a main frequency peak at $f_1 = 53.27$ d^{-1}. This pulsation frequency was also detected in the *BI* bands with $S/N = 4.2$. Amplitude ratios between different bands (ΔB = 10.7 mmag $> \Delta V$ = 8.5 mmag $> \Delta I >$ 6.2 mmag and $\frac{\Delta B}{\Delta V}$ = 1.25, $\frac{\Delta I}{\Delta V}$ = 0.72) are in good agreement with those typical of δ Scuti-type pulsations (Garrido et al. 1990; Rodríguez et al. 1996; Balona & Evers 1999; Rodríguez 2005). In these papers, it can be seen how the amplitude ratios for light curves observed in different photometric bands in a pulsating star mainly depend on the variations in temperature and gravity during the pulsational cycles. This means that they mainly depend on the variations of

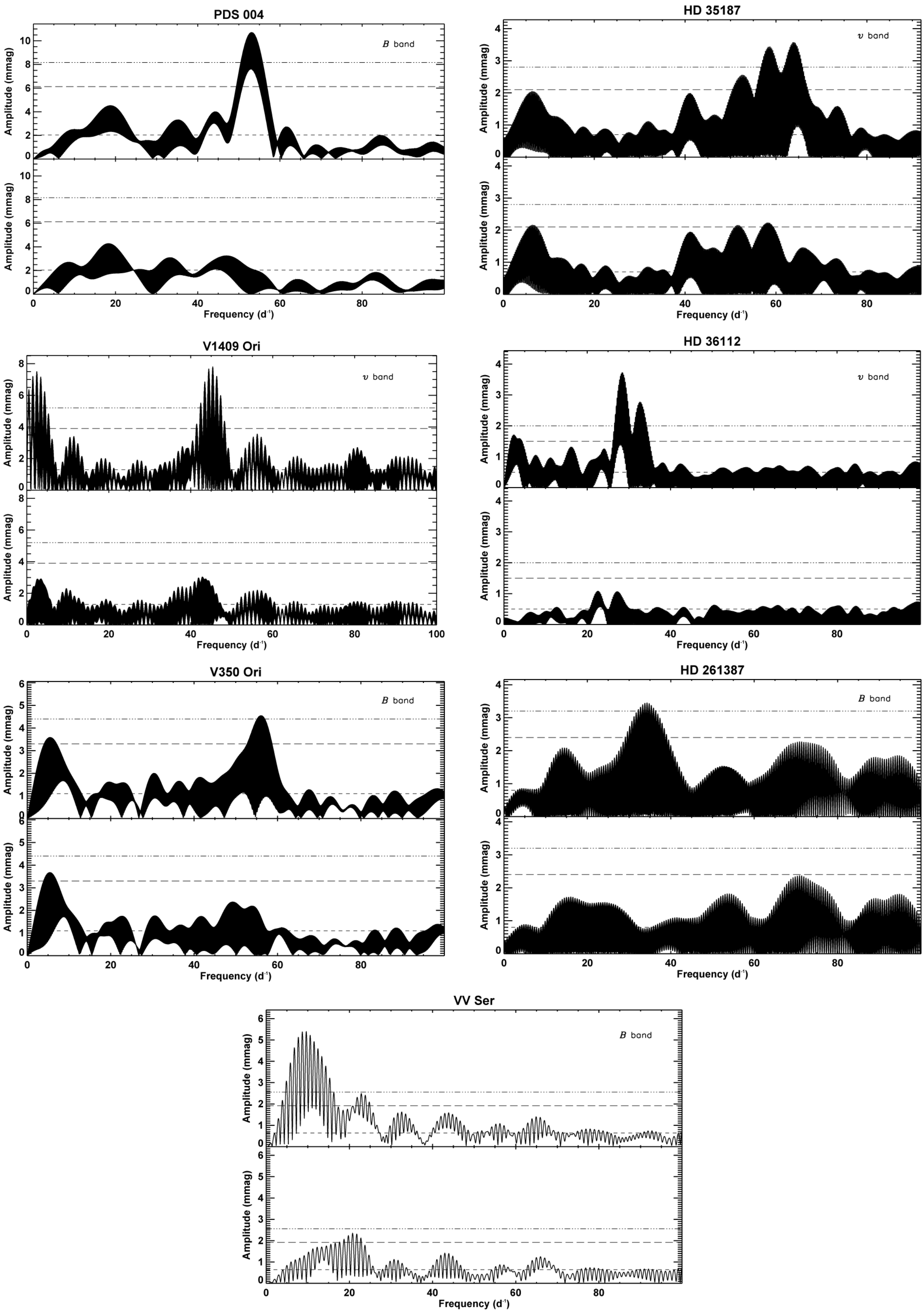

Fig. 1. Frequency analysis in the *v* or *B* bands of the δ Scuti-type stars detected or confirmed in our sample. The dashed, long-dashed, and dot-dashed lines show the σ, 3σ, and 4σ levels, respectively. *Bottom panels*: residuals after prewhitening the main frequency peak detected (see Table 4).

Table 4. PMS and HAEBE stars in which δ Scuti-type pulsation have been detected (ID 3, 9, 14, 15, and 26) or confirmed (ID 63 and 42).

ID number	Name	Spectral Type	Frequency (d^{-1})	ΔB	ΔV	ΔI	Δu (mmag)	Δv	Δb	Δy	Pulsation
3	PDS 004	A1	53.27 (1)	10.7 (7)	8.5 (7)	6.2 (7)	–	–	–	–	δ Scuti
9	HD 35187	A2e	63.87 (1)	–	–	–	3.6 (7)	3.3 (4)	3.1 (4)	2.5 (4)	δ Scuti
14	V1409 Ori	AIab	45.35 (1)	–	–	–	7.6 (11)	7.8 (7)	6.4 (5)	5.4 (7)	δ Scuti
15	HD 36112	A3e	28.36 (1)	–	–	–	3.0 (6)	3.7 (3)	3.5 (3)	2.8 (3)	δ Scuti
26	V350 Ori	A0	57.08 (1)	4.5 (5)	3.3 (4)	3.0 (4)	–	–	–	–	δ Scuti
63	HD 261387	A2V	34.67 (1)	3.5 (3)	2.7 (3)	2.3 (3)	–	–	–	–	δ Scuti
42	VV Ser	A2e	9.65 (4)	5.8 (5)	2.8 (4)	2.6 (6)	–	–	–	–	δ Scuti

these physical parameters in a colour–colour grid, such as (c_1, $(b-y)$) or (c_1, β) grids, but it is not expected to depend (at least not largely) on its evolutionary status as a MS or PMS star.

4.2. HD 35187

The star HD 35187 was observed from October–December 2007 (9.87 h) and December 2009 (1.41 h) using T90 and Strömgren *uvby* bands. It shows a main frequency peak at $f_1 = 63.87$ d^{-1} with a $S/N = 4.7$. The amplitude ratios between different *vby* bands ($\Delta v = 3.3$ mmag $> \Delta b = 3.1$ mmag $> \Delta y = 2.5$ mmag and $\frac{\Delta b}{\Delta y} = 1.24$, $\frac{\Delta v}{\Delta y} = 1.32$) agree well with a δ Scuti-type pulsation. On the other hand, $f_2 = 57.45$ d^{-1} and $f_3 = 6.00$ d^{-1} frequencies show peaks with amplitudes between the 3σ and 4σ significance levels. The frequency f_2 is detected in 2007 and 2009 data but f_3 appears only in 2007 data. This leads us to consider f_3 as only suspect.

4.3. V1409 Ori

The object V1409 Ori was observed with T90 and Strömgren *uvby* bands during four nights: October 2007 (4.94 h), November 2007 (5.94 h) and December 2009 (4.07 h). It shows a short period pulsation at $f_1 = 45.35$ d^{-1}. This frequency is observed in *vby* bands with amplitudes larger than the significance level 4σ. In the case of the *u* band, this peak centred at 45.35 d^{-1} is also detected but with an amplitude below the 3σ significance level due to the high dispersion in the data at this particular band ($\Delta u = 7.6 \pm 1.1$ mmag). Amplitude ratios at this frequency also agree well with a δ Scuti-type pulsation ($\Delta v = 7.8$ mmag $> \Delta b = 6.4$ mmag $> \Delta y = 5.4$ mmag and $\frac{\Delta b}{\Delta y} = 1.18$, $\frac{\Delta v}{\Delta y} = 1.44$).

4.4. HD 36112

The star HD 36112 was observed with T90 and Strömgren *uvby* bands for four nights (9.70 h between October and December 2007 and 8.32 h in December 2009). It shows two peaks above the 4σ level at frequencies $f_1 = 28.36$ d^{-1} and $f_2 = 33.00$ d^{-1}. These frequencies were detected in all *uvby* Strömgren bands. Amplitude ratios between bands at f_1 are characteristic of a δ Scuti-type pulsation ($\Delta v = 3.7$ mmag $> \Delta b = 3.5$ mmag $> \Delta y = 2.8$ mmag $\simeq \Delta u = 3.0$ mmag and $\frac{\Delta b}{\Delta y} = 1.25$, $\frac{\Delta v}{\Delta y} = 1.32$). After prewhitening of f_1 and f_2, residuals show two peaks at $f_3 = 2.62$ d^{-1} and $f_4 = 3.22$ d^{-1} with $S/N > 3.0$. These peaks are most probably generated by a gradient between the two observing nights on October 4 and 9, 2007, which are caused by a bad extinction correction.

4.5. V350 Ori

The object V350 Ori was observed using T150 in the Johnson-Cousins *BVI* bands during four nights, two in January 2008 (5.24 h) and another two in November 2008 (2.23 h). It shows a main frequency peak located at $f_1 = 57.08$ d^{-1} with $S/N = 3.7$. As mentioned in Sect. 3, the TRIPP software showed this peak with a probability >99%, suggesting it as a real peak. The same peak at $f_1 = 57.08$ d^{-1} is also observed in *BI* bands with $S/N = 3.9$ and $S/N = 3.7$, respectively, with a probability >99%. All this suggests that the peak f_1 is real. Moreover, the amplitudes corresponding to different bands are in good agreement with δ Scuti-type pulsations ($\Delta B = 4.5$ mmag $> \Delta V = 3.3$ mmag $> \Delta I = 3.0$ mmag and $\frac{\Delta B}{\Delta V} = 1.36$, $\frac{\Delta I}{\Delta V} = 0.9$).

4.6. HD 261387

The star HD 261387 has already proved to be a δ Scuti-type pulsator by observations carried out using the MOST satellite (Walker et al. 2003) between December 2006 and January 2007 and has been published by Zwintz et al. (2009). The star was included in our study to confirm these findings and support them with new observations. It was observed with both T90 and T150 telescopes and the Strömgren *uvby* and Johnson *BVI* bands, respectively. In the first case, it was observed for only one night in December 2007 for 6.87 h. In the second case, it was observed during four different nights: two nights in January 2008 for 6.14 h, one night in November 2008 for 2.98 h, and one last night in April 2010 for 2.40 h. Frequency analysis shows a peak located at $f_1 = 34.67$ d^{-1} with amplitude $\Delta V = 2.7$ mmag and $S/N = 4.5$. The same peak is observed in the *B* band with an amplitude $\Delta B = 3.5$ mmag and $S/N = 4.0$, which fulfills the amplitude ratio $\frac{\Delta B}{\Delta V} = 1.29$ and agrees well with a δ Scuti-type pulsation. In the case of Johnson *I* band, we have found a peak at the same frequency $f_1 = 34.67$ d^{-1}, which is not significant (<3σ level) due to the higher noise level present in the periodograms for this band.

4.7. VV Ser

The star VV Ser was observed using T150 and *BVI* bands for three nights in April 2007 for a total observing time of 7.01 h and for another night in April 2010 for 1.75 h. For the first time, Ripepi et al. (2007) detected that VV Ser pulsates as a δ Scuti through observations carried out for three consecutive years (2002–2004). For the best data set, which corresponds to 2004, these authors detected seven different pulsation frequencies with values between 2.69 and 10.24 d^{-1}. In our case, we have detected a main frequency peak at $f_1 = 9.65$ d^{-1} that is very probably related to the frequencies $f_5 = 9.55$ d^{-1} (2002 data set), $f_5 = 8.50$ d^{-1} (2003 data set), and $f_6 = 7.56$ d^{-1} (2004 data set),

Table 5. Herbig Be stars in which probable β Cephei-type pulsation have been detected.

ID number	Name	Spectral Type	Frequency (d^{-1})	ΔB	ΔV	ΔI	Δu	Δv	Δb	Δy	Pulsation
				(mmag)							
44	HD 174571	B1.5V	4.51 (1)	–	–	–	5.5 (8)	4.7 (4)	4.6 (4)	3.5 (4)	β Cephei?
50	V1685 Cyg	B3	7.10 (1)	5.7 (6)	4.0 (3)	2.0 (4)	–	–	–	–	β Cephei?
35	HD 50083	B2III	6.45 (1)	–	–	–	3.4 (5)	2.7 (3)	2.7 (3)	2.7 (4)	β Cephei?

Table 6. MS comparison and check stars in which δ Scuti or γ Doradus-type pulsation have been detected.

Name	V (mag)	Spectral Type	Frequency (d^{-1})	Δv (mmag)	Season	Hours (nights)	Points	Pulsation	ID number
HD 202901	8.350	F0	19.00 (7)	4.0 (6)	Aug.09	11.45 (2)	94	δ Scuti	51, 52
HD 203573	7.795	F0	16.20 (3)	23.3 (4)	Aug.09	8.31 (1)	124	δ Scuti	51, 52
			14.41 (3)	19.8 (4)					
HD 35909	6.390	A4	25.61 (10)	14.0 (5)	Oct.07	5.01 (1)	70	δ Scuti	58
HD 37594	5.990	A8	2.80 (9)	14.3 (5)	Dec.07	5.42 (1)	65	γ Dor	13, 19, 26
HD 52343	8.358	F0	3.69 (1)	26.0 (9)	Feb.08	8.41 (2)	54	γ Dor	36, 37, 38, 39, 40, 62

which are detected by Ripepi et al. (2007). Therefore, we can confirm VV Ser as a δ Scuti-type pulsator.

5. β Cephei stars

Three stars are probably β Cephei-type pulsators (HD 174571, V1658 Cyg, and HD 50083). The results are summarised in Table 5. Frequency and amplitude errors are indicated in the parentheses. Figure 2 shows the results of the frequency analysis performed in the v or B bands for these stars. It is important to note that stars more massive than about 8 $M_{\odot}$ do not have an optically visible PMS phase, as the birthline intersects the ZAMS at about this mass (Palla & Stahler 1990). The objects HD 174571, V1658 Cyg, and HD 50083 are classified as early B stars (M > 8 $M_{\odot}$); hence, they are probably young MS stars. On the other hand, it is necessary to obtain more observations to confirm their β Cephei nature.

5.1. HD 174571

The object HD 174571 is a B1.5V star (Frémat et al. 2006). This star was observed on four different nights (May to July 2007, August 2009, and April 2010) with T90 and Strömgren *uvby* bands for a total time of 14.12 h. It shows a main frequency peak located at $f_1 = 4.51$ d^{-1} in all Strömgren bands with amplitudes larger than the 4σ level. Amplitudes in different bands (Δu = 5.5 mmag > Δv = 4.7 mmag > Δb = 4.6 mmag > Δy = 3.5 mmag) are consistent with a β Cephei-type pulsation (Rodríguez 2005).

5.2. V1685 Cyg

The object V1685 Cyg is a B3 star (Manoj et al. 2006; Hernández et al. 2004). With T150, it was observed in the Johnson-Cousins *BVI* bands for one night in August 2007 (4.83 h) and two nights in August 2009 for a total time of 5.24 h. It shows a main frequency peak located at $f_1 = 7.10$ d^{-1} in all Johnson-Cousins *BVI* bands. Amplitudes in different bands (ΔB = 5.7 mmag > ΔV = 4.0 mmag > ΔI = 2.0 mmag) suggest that the variations detected are also caused by β Cephei-type pulsations, which agrees well with its spectral type B3 and main pulsation frequency.

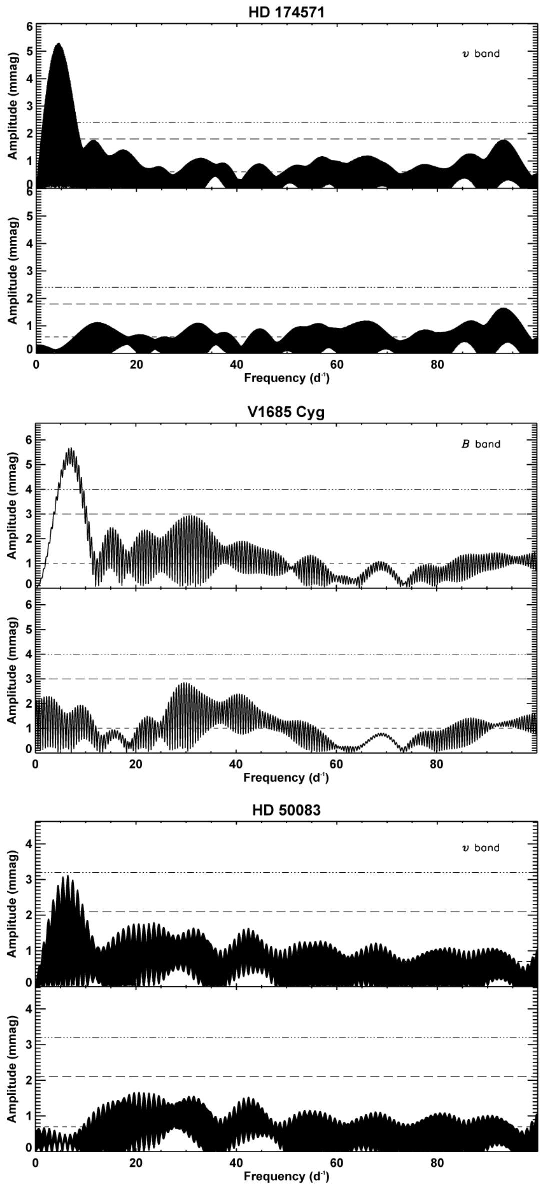

Fig. 2. Frequency analysis in the v or B bands of the β Cephei-type stars detected. The dashed, long-dashed, and dot-dashed lines show the σ, 3σ, and 4σ levels, respectively. *Bottom panels*: residuals after prewhitening the main frequency peak detected (see Table 5).

Table 7. Dereddened photometric indices for the sample of observed stars.

ID number	Name	Spectral type group	V (mag)	$(b-y)$ (mag)	m_1 (mag)	c_1 (mag)	$E(b-y)$ (mag)	$(b-y)_0$ (mag)	m_0 (mag)	c_0 (mag)	δm_1 (mag)	δc_1 (mag)	β (mag)	β^* (mag)	Note
1	VX Cas	B	11.262	0.206	0.068	1.130	0.217	−0.011	0.137	1.087	0.045	…	2.913	…	
2	V594 Cas	B	10.983	0.464	−0.057	0.258	0.587	−0.123	0.126	−0.073	−0.047	…	2.469	2.600	
3	PDS 004	A-F	10.930	0.241	0.144	0.948	0.144	0.097	0.191	0.919	0.017	0.073	2.839	…	
4	XY Per	A0-A3	9.486	0.340	0.122	1.238	0.275	0.065	0.210	1.183	−0.002	0.315	2.850	…	1
5	AB Aur	A0-A3	6.740	0.108	0.120	1.003	0.051	0.057	0.136	0.993	0.069	0.191	2.811	…	
6	HD 31648	A-F	7.384	0.117	0.178	0.944	0.010	0.107	0.181	0.942	0.026	0.118	2.825	…	
9	HD 35187	A-F	7.889	0.171	0.157	0.830	0.021	0.150	0.164	0.826	0.035	0.074	2.786	…	
10	HD 287823	A0-A3	9.867	0.092	0.171	0.899	0.036	0.056	0.182	0.892	0.025	−0.028	2.875	…	
12	HD 290409	A0-A3	10.069	0.055	0.166	1.015	0.048	0.007	0.182	1.006	0.015	0.026	2.919	…	
13	HD 290500	A-F	11.052	0.227	0.121	0.111	0.750	0.116	0.157	0.728	0.051	−0.118	2.838	…	2
14	V1409 Ori	A-F	10.201	0.118	0.192	0.870	0.000	0.118	0.192	0.870	0.010	0.240	2.736	…	3
15	HD 36112	A-F	8.466	0.180	0.181	0.880	0.058	0.122	0.200	0.868	0.006	0.057	2.816	…	
16	V1410 Ori	A-F	9.502	0.099	0.193	0.986	0.016	0.083	0.198	0.983	0.010	0.117	2.849	…	
17	HD 36408	B	5.379	0.046	0.075	0.762	0.090	−0.044	0.104	0.744	0.012	…	2.704	…	
18	V1271 Ori	A0-A3	9.793	0.056	0.135	0.839	0.007	0.049	0.137	0.838	0.047	0.159	2.749	…	
19	V380 Ori	G	10.463	0.365	0.030	0.282	…	…	…	…	…	…	2.359	…	4
20	HD 290770	B	9.196	0.028	0.116	0.869	0.061	−0.033	0.135	0.857	−0.005	…	2.741	…	
21	BF Ori	A0-A3	11.072	0.267	0.157	1.221	0.232	0.035	0.231	1.175	−0.026	0.233	2.892	…	
22	HD 37357	A0-A3	8.858	0.069	0.169	0.975	0.022	0.047	0.176	0.971	0.031	0.065	2.868	…	
23	V1247 Ori	A-F	10.176	0.193	0.213	0.831	0.000	0.193	0.213	0.831	−0.029	0.273	2.712	…	6
24	V1788 Ori	A0-A3	9.815	0.102	0.164	1.009	0.043	0.059	0.178	1.000	0.029	0.068	2.884	…	
25	RR Tau	…	…	…	…	…	…	…	…	…	…	…	…	…	5
26	V350 Ori	A0-A3	10.879	0.149	0.247	1.169	0.108	0.041	0.282	1.147	−0.079	0.196	2.900	…	7
27	HD 37806	B	7.650	0.059	0.086	0.838	0.096	−0.037	0.117	0.819	0.003	…	2.713	…	
28	HD 38120	B	8.810	0.044	0.119	0.949	0.069	−0.025	0.141	0.935	−0.030	…	2.692	…	
30	HD 249879	B	10.253	0.041	0.122	0.876	0.073	−0.032	0.146	0.861	−0.004	…	2.775	…	
31	V791 Mon	B	10.429	0.242	0.013	0.320	0.357	−0.115	0.122	0.009	−0.034	…	2.462	2.620	
32	HD 250550	B	9.175	0.082	0.085	0.624	0.140	−0.058	0.130	0.596	−0.035	…	2.654	…	
33	AE Lep	A-F	10.006	0.103	0.118	0.925	0.008	0.095	0.121	0.923	0.087	0.070	2.842	…	
34	PDS 126	A0-A3	12.089	0.321	0.126	0.954	0.271	0.050	0.213	0.900	−0.009	−0.050	2.899	…	
35	HD 50083	B	6.958	0.104	−0.002	−0.039	0.248	−0.144	0.073	−0.293	…	…	2.440	2.530	4
36	HD 52721	B	6.369	0.098	0.029	0.001	0.225	−0.127	0.099	−0.113	0.058	…	2.562	2.589	
37	HT Cma	B	11.819	0.327	0.022	1.033	0.350	−0.023	0.134	0.963	0.010	…	2.796	…	
38	HU Cma	B	12.161	0.255	−0.010	0.647	0.306	−0.081	0.092	0.359	0.022	…	2.514	2.700	
39	HD 53367	B	7.258	0.369	−0.072	−0.049	0.506	−0.137	0.088	−0.222	…	…	2.543	2.550	4
40	PDS 241	B	12.176	0.443	−0.032	−0.048	0.575	−0.132	0.152	−0.163	…	…	1.657	…	4
41	HD 141569	A0-A3	7.122	0.123	1.005	0.083	0.052	0.031	0.140	0.995	0.068	0.122	2.853	…	
42	VV Ser	B	12.342	0.618	0.015	0.720	0.677	−0.059	0.232	0.585	−0.155	…	2.603	…	
43	V431 Sct	B	12.769	0.805	−0.194	0.006	0.961	−0.156	0.108	−0.411	…	…	2.401	2.480	4
44	HD 174571	B	9.109	0.498	−0.153	0.328	0.605	−0.107	0.038	0.093	0.049	…	2.558	2.640	
45	HD 179218	A0-A3	7.084	0.079	0.117	1.141	0.047	0.032	0.132	1.132	0.076	0.269	2.847	…	
46	WW Vul	A-F	10.947	0.264	0.171	1.002	0.151	0.113	0.219	0.972	−0.013	0.155	2.819	…	
47	PX Vul	A-F	12.214	0.423	0.025	0.347	0.133	0.290	0.068	0.320	0.119	−0.039	2.635	…	2
48	PDS 581	B	12.037	0.511	0.109	0.079	0.686	−0.175	0.316	−0.614	…	…	2.120	2.370	4
49	HD 190073	A0-A3	7.619	0.090	0.097	1.059	0.015	0.075	0.102	1.056	0.068	0.590	2.680	…	1
50	V1685 Cyg	B	11.506	0.597	−0.119	−0.219	0.768	−0.171	0.122	−0.565	…	…	2.384	2.400	4
51	HD 200775	B	7.415	0.319	−0.008	0.102	0.449	−0.130	0.132	−0.143	…	…	2.499	2.580	4
52	HD 203024	A-F	8.652	0.121	0.138	0.906	0.006	0.115	0.140	0.905	0.067	0.086	2.820	…	
53	BD +65.1637	B	10.151	0.356	−0.047	0.210	0.474	−0.118	0.102	−0.022	−0.020	…	2.528	2.610	
54	V1578 Cyg	B	10.124	0.296	0.071	0.977	0.324	−0.028	0.175	0.912	−0.066	…	2.687	…	
55	BH Cep	A-F	11.217	0.406	0.141	0.518	0.150	0.256	0.189	0.488	−0.017	−0.025	2.695	…	
56	SV Cep	A0-A3	11.083	0.257	0.089	0.940	0.196	0.061	0.139	0.909	0.067	−0.025	2.885	…	
57	V1080 Tau	G	11.186	0.828	−0.087	0.546	…	…	…	…	…	…	2.567	…	4
58	CO Ori	G	11.452	0.540	0.287	0.085	…	…	…	…	…	…	2.596		4
59	V1650 Ori	A-F	10.726	0.436	0.162	0.103	0.333	0.195	0.413	−0.010	0.048	2.638	…		
60	RY Ori	A-F	12.416	0.549	0.162	0.434	0.338	0.387	0.390	0.085	−0.215	−0.325	2.658	…	
61	HD 36910	A-F	10.334	0.429	0.214	0.781	0.244	0.185	0.292	0.732	−0.097	−0.004	2.778	…	7
62	HD 53240	B	6.120	−0.008	0.087	0.844	0.027	−0.035	0.096	0.839	0.006	…	2.671	…	
63	HD 261387	A0-A3	10.534	0.093	0.181	0.971	0.027	0.066	0.190	0.966	0.017	0.047	2.874	…	

Notes. (1) High luminosity, $\delta c_1 \geq 0.^m28$; (2) low metallicity subluminous star, (3) Ap star with $E(b-y) \leq -0.^m04$ (derived value was $E(b-y) = -0.^m065$, adopted value is $E(b-y) = 0.^m000$); (4) out of calibration range (Philip & Egret 1980); (5) $uvby\beta$ photometry was not collected for this star; (6) derived value was $E(b-y) = -0.^m028$, adopted value $E(b-y) = 0.^m000$; (7) Am star, $m_0 > 0.^m22$.

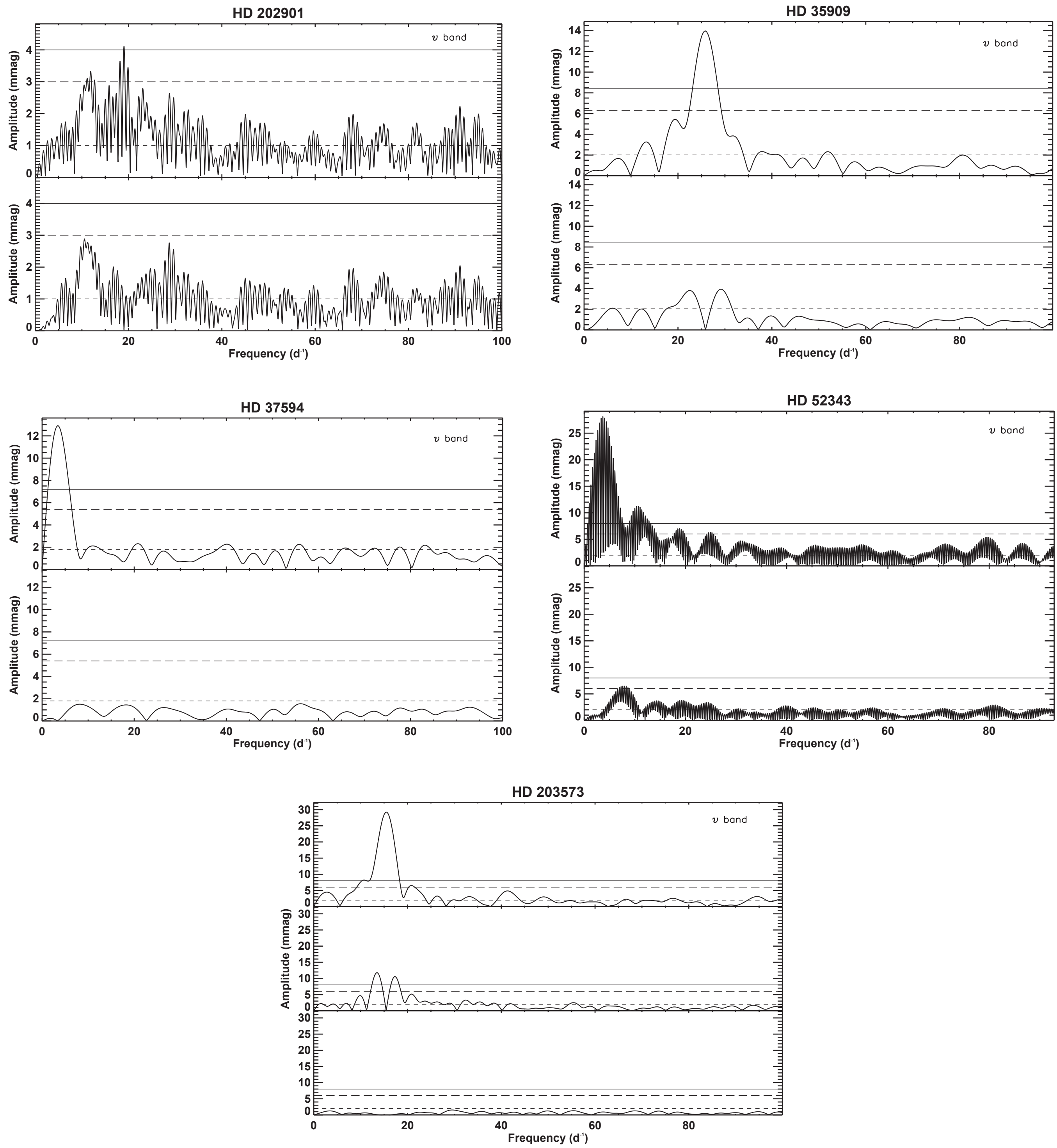

Fig. 3. Frequency analysis in the v band of the MS comparison and check stars in which δ Scuti or γ Doradus-type pulsation have been detected. The dashed, long-dashed, and dot-dashed lines show the σ, 3σ, and 4σ levels, respectively. *Bottom panels*: residuals after prewhitening the main frequency peak detected (see Table 6).

5.3. HD 50083

The star HD 50083 was observed using the T90 and Strömgren *uvby* bands during two nights in December 2007 (5.36 h) for one night in February 2010 (2.85 h) and another one in February 2010 (3.08 h). It shows a main frequency peak located at f_1 = 6.45 d^{-1} for the v band with S/N = 3.8 and a probability >99%, suggesting this as a real peak. Moreover, this peak is present in all Strömgren bands with amplitudes Δu = 3.4 mmag > Δv, Δb, Δy = 2.7 mmag, and $\frac{\Delta v}{\Delta u}$ = 0.79, which suggests β Cephei-type pulsations, according to its spectral type B2III (Frémat et al. 2006) and pulsation frequency.

6. Stellar physical parameters

Stellar physical parameters were determined using the colour and β indices from Strömgren photometry collected in this work. To obtain the dereddened indices $(b-y)_0$, m_0, and c_0,

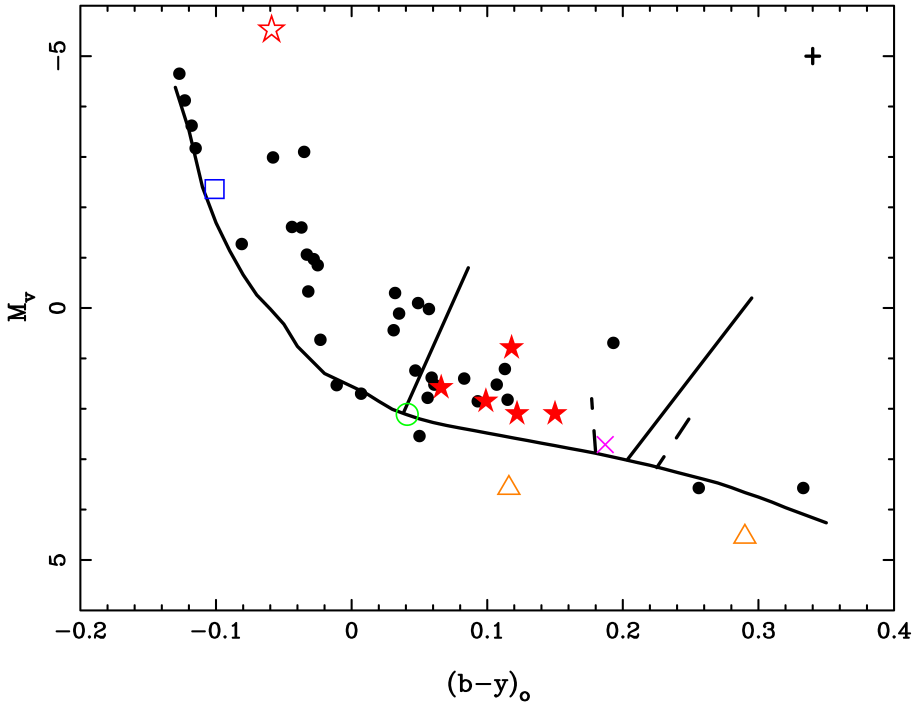

Fig. 4. Colour−magnitude diagram of the sample of observed stars. Observational edges for the MS δ Scuti instability region (solid lines) are from Rodríguez & Breger (2001) and those for the γ Dor region (dashed lines) are from Handler & Shobbrook (2002). Red solid asterisks: PMS δ Scuti-type stars (PDS 004, HD 35187, V1409 Ori, HD 36112, and HD 261387); black solid circles: constant stars; green open circle: V350 Ori (δ Scuti-type Am star); blue open square: HD 174571 (probable β Cephei-type pulsator); red open asterisk: VV Ser (δ Scuti-type star, see text for explanation); orange open triangles: subluminous stars (HD 290500 and PX Vul); and magenta cross: HD 36910 (Am star). Upper right: error bars.

an initial classification of the stars in their different spectral groups was first necessary. For this purpose, the spectral classification given by Strömgren (1966) was used. Once the stars were classified, photometric indices were dereddened by following the equations and ZAMS reference lines derived by Philip & Egret (1980). Stars previously classified in the literature as Be stars were dereddened using the method developed by Fabregat & Torrejón (1998). Table 7 shows the spectral type group; visual magnitude V; photometric indices $(b-y)$, m_1, and c_1; and the dereddened indices $(b-y)_0$, m_0, c_0, δm_1, and δc_1. The last two columns show the β values, and the modified β^* values obtained using the method developed by Fabregat & Torrejón (1998) in the case of Be stars. Typical error bars are about $0\overset{m}{.}01$ for E$(b-y)$, $(b-y)_0$, m_0, c_0, δm_1, and $0\overset{m}{.}02$ for δc_1. In the particular case of Be stars, typical error bars are about $0\overset{m}{.}04$ for all indices. For 33 stars of the sample, there was no *uvbyβ* photometry available in the literature. For all the remaining stars, the *uvbyβ* indices are listed in the catalogue of Hauck & Mermilliod (1998). Their values are in good agreement within the error bars with our results.

To obtain the effective temperature ($T_{\rm eff}$), surface gravity (log g), and [Fe/H] values, different grids were used depending on the aforementioned spectral classification: NEMO-2004 CGM grids (Nendwich et al. 2004) for A-F stars (5500 K $\leq T_{\rm eff} \leq$ 8500 K, late group), the grids of Moon & Dworetsky (1985) with the log g corrections suggested by Napiwotzki et al. (1993) for A0-A3 stars (8500 K $< T_{\rm eff} \leq$ 11 000 K, intermediate group), and the Napiwotzki et al. (1993) grids for the B group (11 000 K $< T_{\rm eff} \leq$ 35 000 K, early group). Table 8 lists the fundamental physical parameters for the sample stars: name, absolute magnitude, effective temperature, log g, metallicity, spectral type group, and calibration used. Typical error bars for log g are about 0.25 dex for stars with $T_{\rm eff} >$ 20 000 K, ≈0.15 dex for stars with 11 000 $\leq T_{\rm eff} \leq$ 20 000 K, and ≈0.10 dex for $T_{\rm eff} \leq$ 11 000 K. In the case of $T_{\rm eff}$, relative errors in its determination are about 4% for $T_{\rm eff} >$ 20 000 K, 3% for 11 000 $\leq T_{\rm eff} \leq$ 20 000 K, and 2.5% for $T_{\rm eff} \leq$ 11 000 K (Napiwotzki et al. 1993). Typical errors in the determination of M_V and [Fe/H] are about $0.^m3$ (Crawford 1975, 1978, 1979) and 0.1 dex (Nissen 1988; Smalley 1993), respectively.

Although the dereddening procedure and photometric calibrations used are a well-proven method to obtain the stellar parameters for MS stars, they might not be correct for some HAEBE stars depending on the amount of circumstellar material. For this reason, the stellar parameters obtained must be considered just as an initial estimate and need to be checked with future spectroscopic observations.

Figure 4 shows a colour-magnitude diagram, where our sample of observed PMS and HAEBE stars has been placed. The observational instability region for MS δ Scuti-type stars (Rodríguez & Breger 2001) with that of γ Dor variables (Handler & Shobbrook 2002) are also shown. Zwintz (2008) compared the observational instability regions for pulsating PMS and classical (post- and MS) δ Scuti-type stars, making use of the sample of PMS pulsators available up to that date, and concluded that the hot and cool borders of both instability regions seem to coincide. Our results seems to be also in good agreement with this finding, as we show below.

All five PMS δ Scuti-type stars detected in this work (PDS 004 (ID 3), HD 35187 (ID 9), V1409 Ori (ID 14), HD 36112 (ID 15), and V350 Ori (ID 26)) are placed within the limits of the observational instability strip for the classical δ Scuti stars. We note that V350 Ori is located just on the locus of the MS and very close to the blue edge. However, it has been classified as an Am star in Table 7. Rodríguez & Breger (2001) showed that absolute magnitudes obtained with

Table 8. Fundamental physical parameters for the sample of observed stars.

ID number	Name	M_V (mag)	$T_{\rm eff}$ (K)	log g	[Fe/H]	Spectral type group	Calibration adopted
		±0.3			±0.1		
1	VX Cas	1.5	9850 ± 250	4.07 ±0.10	–	A0-A3	3
2	V594 Cas	−4.1	30 500 ± 1000	4.05 ± 0.25	–	B	2
3	PDS 004	1.9	8030 ± 200	4.18 ± 0.10	−0.10	A	1
4	XY Per	–	–	–	–	–	–
5	AB Aur	0.0	8780 ± 200	3.64 ± 0.10	−0.65	A0-A3	3
6	HD 31648	1.5	7870 ± 200	4.02 ± 0.10	−0.19	A	1
9	HD 35187	2.1	7490 ± 200	4.07 ± 0.10	−0.29	A	1
10	HD 287823	1.8	8740 ± 200	4.35 ± 0.10	−0.18	A0-A3	3
12	HD 290409	1.7	9440 ± 250	4.27 ± 0.10	–	A0-A3	3
13	HD 290500	3.6	7700 ± 200	>4.50	−0.46	A	1
14	V1409 Ori	0.8	7820 ± 200	4.19 ± 0.10	−0.02	A	1
15	HD 36112	2.1	7770 ± 200	4.16 ± 0.10	0.02	A	1
16	V1410 Ori	1.4	8140 ± 200	4.06 ± 0.10	−0.02	A	1
17	HD 36408	−1.6	11 950 ± 350	3.22 ± 0.15	–	B	2
18	V1271 Ori	−0.1	9310 ± 250	3.56 ± 0.10	–	A0-A3	3
19	V380 Ori	–	–	–	–	–	–
20	HD 290770	−1.1	11 300 ± 350	3.41 ± 0.15	–	B	2
21	BF Ori	0.1	8600 ± 200	3.67 ± 0.10	0.35	A0-A3	1
22	HD 37357	1.2	8790 ± 200	4.09 ± 0.10	−0.25	A0-A3	3
23	V1247 Ori	0.7	7060 ± 200	3.64 ± 0.10	0.55	F	1
24	V1788 Ori	1.4	8470 ± 200	4.16 ± 0.10	−0.22	A0-A3	1
25	RR Tau	–	–	–	–	–	–
26	V350 Ori	2.1	8500 ± 200	3.74 ± 0.10	0.91	A0-A3	1
27	HD 37806	−1.6	11 500 ± 350	3.18 ± 0.15	–	B	2
28	HD 38120	−0.9	10 700 ± 250	2.66 ± 0.10	–	B	3
30	HD 249879	−0.3	11 350 ± 350	3.68 ± 0.15	–	B	2
31	V791 Mon	−3.2	25 600 ± 1000	4.07 ± 0.25	–	B	2
32	HD 250550	−3.0	12 800 ± 350	2.81 ± 0.15	–	B	2
33	AE Lep	1.9	8050 ± 200	4.18 ± 0.10	−0.84	A	1
34	PDS 126	2.5	8650 ± 200	4.50 ± 0.10	0.18	A0-A3	1
35	HD 50083	–	–	–	–	–	–
36	HD 52721	−4.7	33 800 ± 1500	4.21 ± 0.25	–	B	2
37	HT Cma	0.6	10 560 ± 250	3.61 ± 0.10	–	B	3
38	HU Cma	−1.3	16 000 ± 500	4.15 ± 0.15	–	B	2
39	HD 53367	–	–	–	–	–	–
40	PDS 241	–	–	–	–	–	–
41	HD 141569	0.4	9220 ± 250	3.93 ± 0.10	−0.64	A0-A3	3
42	VV Ser	−5.5	12 150 ± 350	2.06 ± 0.15	–	B	2
43	V431 Sct	–	–	–	–	–	–
44	HD 174571	−2.4	22 700 ± 1000	4.13 ± 0.25	–	B	2
45	HD 179218	−0.3	8930 ± 200	3.55 ± 0.10	−0.72	A0-A3	3
46	WW Vul	1.2	7770 ± 200	3.87 ± 0.10	0.22	A	1
47	PX Vul	4.5	6120 ± 150	>4.50	−1.18	F	1
48	PDS 581	–	–	–	–	–	–
49	HD 190073	–	–	–	–	–	–
50	V1685 Cyg	–	–	–	–	–	–
51	HD 200775	–	–	–	–	–	–
52	HD 203024	1.8	7820 ± 200	4.09 ± 0.10	−0.63	A	1
53	BD +65.1637	−3.6	27 200 ± 1000	3.99 ± 0.25	–	B	2
54	V1578 Cyg	−1.0	10 830 ± 250	2.66 ± 0.10	–	B	2
55	BH Cep	3.6	6750 ± 150	4.50 ± 0.10	0.36	F	1
56	SV Cep	1.5	8830 ± 200	4.39 ± 0.10	−0.63	A0-A3	3
57	V1080 Tau	–	–	–	–	–	–
58	CO Ori	–	–	–	–	–	–
59	V1650 Ori	3.6	6170 ± 150	4.25 ± 0.10	0.23	F	1
60	RY Ori	7.1	5810 ± 150	>4.50	2.72	F	1
61	HD 36910	2.8	7230 ± 200	4.11 ± 0.10	1.10	F	1
62	HD 53240	−3.1	11 100 ± 350	2.57 ± 0.15	–	B	2
63	HD 261387	1.6	8400 ± 200	4.23 ± 0.10	−0.10	A0-A3	1

Notes. Calibrations adopted: 1: NEMO-2004 CGM (Nendwich et al. 2004; Heiter et al. 2002). Late group, the parameters $(b-y)_0$ and c_0 are used here as temperature and luminosity indicators, respectively. 2: Napiwotzki et al. (1993). Early group, the parameters c_0 and β are used as temperature and luminosity indicators, respectively. 3: Moon & Dworetsky (1985). Intermediate group, the parameters a_0 y r^* together with a log g correction (Napiwotzki et al. 1993) are used for this group.

photometric calibrations for Am stars have large systematic errors, underestimating their luminosities in relation to those obtained using distances from HIPPARCOS (Perryman et al. 1997) in all cases. Therefore, V350 Ori must be located above the MS and slightly shifted to the left of the blue edge.

The objects HD 261387 (ID 63) and VV Ser (ID 42) are the two stars with confirmed δ Scuti-type pulsations. The former is also placed inside the classical δ Scuti instability region, but the latter, according to our photometric data and calibrations, is placed in the B supergiant region. This is probably due to an anomalous β index derived from its variable H_β line in emission (Chavarria-K. et al. 1988). However, these authors classified VV Ser as an A2eβ star by means of spectroscopic observations, which place VV Ser within the limits of the δ Scuti region.

Two of the stars with detected β-Cephei-like variability, V1685 Cyg (ID 50) and HD 50083 (ID 35), are not shown in Fig. 4 because their β index, which is used to derive their temperatures, falls outside the limits of the β calibration (Philip & Egret 1980). If used, they should be placed in the B0-B2 region. Concerning HD 174571 (ID 44), this star could be located on the colour-magnitude diagram near the MS and in the early B stars region. Thereby, these three stars are located in the region, where β Cephei-type pulsation can be excited, supporting the possibility that their membership to that group of pulsators is real.

Some stars that do not have any type of pulsation detected present problems concerning their photometric calibrations. The stars HD 53367 (ID 39), PDS 241 (ID 40), V431 Sct (ID 43), HD 200775 (ID 51), PDS 581 (ID 48), V1080 Tau (ID 57), and CO Ori (ID 58) could not be calibrated because their β indices are outside of the range covered by the calibrations used. The first five objects are early B stars, whereas V1080 Tau and CO Ori are G stars. Moreover, PDS 241 and V380 Ori present anomalous β indices very probably due to strong emission in the H_β line (1.657 and 2.359, respectively), which makes it impossible to obtain any reliable β index.

On the other hand, XY Per (ID 4) and HD 190073 (ID 49) are classified as high luminosity stars. There are no appropriate dereddening equations for this type of star, as it has been already indicated by Philip & Egret (1980). Therefore, these stars were rejected from the calibration. The stars HD 290500 (ID 13) and PX Vul (ID 47) appear as subluminous stars due to an insufficient derredening in their photometric indices which is probably caused by the large amount of circumstellar dust present around these stars. Finally, HD 36910 (ID 61) is classified as an Am star located on the MS and close to the red edge of the δ Scuti instability strip. However, its position would be shifted up above the MS because the luminosities obtained by photometric calibrations for Am stars are systematically underestimated, as in the case of V350 Ori.

7. Summary and conclusions

A systematic search for δ Scuti-type pulsations was carried out over a well-defined sample of northern field stars previously classified as either PMS or HAEBE stars. We have detected five new PMS δ Scuti-type stars (PDS 004, HD 35187, V1409 Ori, HD 36112, and V350 Ori) and three probable β Cephei-type pulsators (HD 174571, V1685 Cyg, and HD 50083). In addition, three new MS δ Scuti-type pulsators (HD 202901, HD 203573, and HD 35909) and two MS stars that show γ Doradus-type pulsations (HD 37594 and HD 52343) have also been detected among the comparison and check stars. Finally, two stars (HD 261387 and VV Ser) have also been confirmed as PMS δ Scuti-type pulsators in this work.

The sample of observed stars has been placed in a colour–magnitude diagram, and their stellar physical parameters were derived using Strömgren photometry and photometric calibrations. All five PMS stars that have detected δ Scuti-type pulsation are located within the observational limits of the observational instability strip for the classical δ Scuti stars, which confirms their nature as PMS δ Scuti-type pulsators. Although photometric calibrations are a well-proven method for MS stars, it is important to note that they are not very reliable for some PMS field stars due to their HAEBE nature, which results from the following: emission of the H_β line due to hot gas located in their accretion discs (affecting their β index), presence of a large amount of dust in the circumstellar material (resulting in peculiarities in their colour $(b-y)$ indices), and high accretion rates that produce a luminosity excess in UV (affecting their c_1 index associated to this band) in some cases. Therefore, it is important to obtain spectroscopic observations for these stars to check the physical parameters obtained. Finally, this search for δ Scuti-type pulsations among PMS stars is only a first step to a proper study of their inner layers. With this purpose, it is necessary to obtain new observations of long runs for each star to obtain a more detailed frequency content that will allow to model their inner structure.

Acknowledgements. This work is supported by the Spanish Ministry of Economy and Competitiveness (MINECO) under the grant BES-2007-15372. This work has been partially funded by the projects AYA2006-06375, AYA2009-10394, and AYA2011-30147-C03-01 of the Spanish Ministry of Economy and Competitiveness (MINECO), cofounded with FEDER funds, and 2011 FQM 7363 of the Consejería de Economía, Innovación, Ciencia y Empleo (Junta de Andalucía). This work made use of the SIMBAD database, operated at CDS, Strasbourg, France. We want to thank an anonymous referee for their comments and suggestions which help us to improve this paper. We also thank A. Fernández-Martín for her suggestions and support.

References

Amado, P. J., Moya, A., Suárez, J. C., et al. 2004, MNRAS, 352, L11
Balona, L. A., & Evers, E. A. 1999, MNRAS, 302, 349
Breger, M., & Pamyatnykh, A. A. 1998, A&A, 332, 958
Breger, M., Stich, J., Garrido, R., et al. 1993, A&A, 271, 482
Breger, M., Handler, G., Garrido, R., et al. 1999, A&A, 349, 225
Casey, M. P., Zwintz, K., Guenther, D. B., et al. 2013, MNRAS, 428, 2596
Chavarria-K., C., de Lara, E., Finkenzeller, U., Mendoza, E. E., & Ocegueda, J. 1988, A&A, 197, 151
Crawford, D. L. 1975, AJ, 80, 955
Crawford, D. L. 1978, AJ, 83, 48
Crawford, D. L. 1979, AJ, 84, 1858
Fabregat, J., & Torrejón, J. M. 1998, A&A, 332, 643
Finkenzeller, U., & Mundt, R. 1984, A&AS, 55, 109
Frémat, Y., Neiner, C., Hubert, A.-M., et al. 2006, A&A, 451, 1053
Garrido, R., García-Lobo, E., & Rodríguez, E. 1990, A&A, 234, 262
Grinin, V. P., The, P. S., de Winter, D., et al. 1994, A&A, 292, 165
Guenther, D. B., Kallinger, T., Zwintz, K., Weiss, W. W., & Tanner, J. 2007, ApJ, 671, 581
Guenther, D. B., Kallinger, T., Zwintz, K., et al. 2009, ApJ, 704, 1710
Handler, G., & Shobbrook, R. R. 2002, MNRAS, 333, 251
Hauck, B., & Mermilliod, M. 1998, A&AS, 129, 431
Heiter, U., Kupka, F., van't Veer-Menneret, C., et al. 2002, A&A, 392, 619
Herbig, G. H. 1960, ApJS, 4, 337
Herbig, G. H. 1962, Adv. Astron. Astrophys., 1, 47
Herbst, W., & Shevchenko, V. S. 1999, AJ, 118, 1043
Hernández, J., Calvet, N., Briceño, C., Hartmann, L., & Berlind, P. 2004, AJ, 127, 1682
Joy, A. H. 1945, ApJ, 102, 168
Lenz, P., & Breger, M. 2005, CoAst, 146, 53
Manoj, P., Bhatt, H. C., Maheswar, G., & Muneer, S. 2006, ApJ, 653, 657
Marconi, M., & Palla, F. 1998, ApJ, 507, L141
Montgomery, M. H., & O'Donoghue, D. 1999, Delta Scuti Star Newsletter, 13, 28
Moon, T. T., & Dworetsky, M. M. 1985, MNRAS, 217, 305

Napiwotzki, R., Schoenberner, D., & Wenske, V. 1993, A&A, 268, 653
Nendwich, J., Heiter, U., Kupka, F., Nesvacil, N., & Weiss, W. W. 2004, CoAst, 144, 43
Nissen, P. E. 1988, A&A, 199, 1
Oudmaijer, R. D., Palacios, J., Eiroa, C., et al. 2001, A&A, 379, 564
Palla, F., & Stahler, S. W. 1990, ApJ, 360, L47
Perryman, M. A. C., Lindegren, L., Kovalevsky, J., et al. 1997, A&A, 323, L49
Philip, A. D., & Egret, D. 1980, A&AS, 40, 199
Ripepi, V., Bernabei, S., Marconi, M., et al. 2007, A&A, 462, 1023
Rodríguez, E. 2005, PASPC, 333, 165
Rodríguez, E., & Breger, M. 2001, A&A, 366, 178
Rodríguez, E., Rolland, A., López de Coca, P., & Martín, S. 1996, A&A, 307, 539
Rodríguez, E., González-Bedolla, S. F., Rolland, A., Costa, V., & López de Coca, P. 1997, A&A, 324, 959
Rogers, N.Y. 1995, CoAst, 78
Scargle, J. D. 1982, ApJ, 263, 835
Schuh, S. L., Dreizler, S., Deetjen, J. L., & Goumlhler, E. 2003, Baltic Astron., 12, 167
Smalley, B. 1993, A&A, 274, 391
Stahler, S. W. 1983, ApJ, 274, 822
Strömgren, B. 1966, ARA&A, 4, 433
The, P. S., de Winter, D., & Perez, M. R. 1994, A&AS, 104, 315
Vieira, S. L. A., Corradi, W. J. B., Alencar, S. H. P., et al. 2003, AJ, 126, 2971
Walker, G., Matthews, J., Kuschnig, R., et al. 2003, PASP, 115, 1023
Wenzel, W., Dorschner, J., & Friedemann, C. 1971, Astron. Nachr., 292, 221
Zwintz, K. 2008, ApJ, 673, 1088
Zwintz, K., Hareter, M., Kuschnig, R., et al. 2009, A&A, 502, 239
Zwintz, K., Kallinger, T., Guenther, D. B., et al. 2011, ApJ, 729, 20
Zwintz, K., Fossati, L., Guenther, D. B., et al. 2013, A&A, 552, A68